GeoFlow: On symmetry-breaking bifurcations of heated spherical shell convection

K Bergemann[1], F Feudel[1], L S Tuckerman[2]

[1] Inst. of Physics, University of Potsdam, Am Neuen Palais 10, D-14469 Potsdam, Germany
[2] PMMH-ESPCI, 75231 Paris, France

E-mail: `bergemann@agnld.uni-potsdam.de`

Abstract. Convective motion in a spherical shell under the influence of a central force has been investigated numerically as a part of the GeoFlow experiment which will run under microgravity conditions on the International Space Station (ISS). An approach combining numerical simulations with a spectral time-stepping code and path-following techniques allows the computation of both stable and unstable solution branches of stationary states. The stability of the solutions has been determined by computing the leading eigenvalues of the Jacobian matrix. Additionally, special attention is paid to the symmetry-breaking bifurcations which are controlled by subgroups of the full spherical symmetry group $O(3)$, under which the governing equations and the primary motionless conductive state are invariant. Finally, the transition from the stationary to the time-dependent regime is described.

1. Introduction

The ongoing GeoFlow experiment [1, 2, 3] seeks to investigate thermal convection in a spherical shell under the influence of a central force field for both rotating and nonrotating spheres. By means of the dielectrophoretic effect, a central force field with a $1/r^5$ radial dependence is generated in the experiment. This can be used as an approximate model for the action of gravity within the giant gaseous planets. In addition to its application to planetary atmospheres, the comparison of the theoretical predictions and the experimental realizations could be of great interest to both experimentalists and theorists. In the following, we will treat only the nonrotating case.

The governing equations for the convection of a fluid in a spherical shell with radii $R_2 > R_1$ heated from within and driven by buoyancy due to the central force field are the Boussinesq equations in spherical geometry, which can be cast in the dimensionless form:

$$\mathrm{Pr}^{-1}\left[\frac{\partial \boldsymbol{u}}{\partial t} + (\boldsymbol{u}\cdot\boldsymbol{\nabla})\boldsymbol{u}\right] = -\boldsymbol{\nabla} p + \boldsymbol{\nabla}^2\boldsymbol{u} + \frac{\mathrm{Ra}\,T}{\beta^2 r^5}\boldsymbol{e_r},$$

$$\nabla\cdot\boldsymbol{u} = 0\ , \qquad \frac{\partial T}{\partial t} + \boldsymbol{u}\cdot\boldsymbol{\nabla} T = \boldsymbol{\nabla}^2 T,$$

$$\boldsymbol{u}(R_1) = \boldsymbol{u}(R_2) = \boldsymbol{0}\ , \qquad T(R_1) = 1\ , \qquad T(R_2) = 0,$$

where $\boldsymbol{e_r}$ is the radial unit vector and $\beta = (R_2 - R_1)/R_1$ is the normalized gap size. In the experimental setup the gap size is fixed to $\beta = 1$ (i.e. $R_2 = 2\,R_1$) and the silicone oil used has a

Prandtl number of Pr = 64.64. The Rayleigh number Ra, which is proportional to the applied radial temperature difference, serves as the only control parameter in the nonrotating regime.

The underlying foundation of the numerical tools is a time-stepping spectral solver which is based on a decomposition of the velocity field into poloidal and toroidal potentials [4]. In addition to being used for time-dependent simulations, a biconjugate gradient method is incorporated in order to compute efficiently the stationary solutions [5] via Newton's method. By means of this approach, one can trace the steady states along both the stable and unstable branches, as a function of the Rayleigh number. This paper presents the first results in the construction of a bifurcation diagram describing qualitatively the convective solutions that appear after loss of stability of the conductive solution, prior to the appearance of chaos.

2. Simulations

Using the pseudo-spectral time-stepping code [4] mentioned above, we were able to obtain four qualitatively different steady states. For low Rayleigh numbers, the conductive state is the only steady solution. The fluid is at rest and the spherically symmetric temperature profile is $T(r) \propto \frac{1}{r}$. A linear stability analysis shows that this state becomes unstable at Ra = 2491 and convection sets in, in accordance with the results found by Travnikov [2, 6]. Above this critical Rayleigh number, e.g. at Ra = 2500, the pattern which appears seems to be axisymmetric and the $(l = 4, m = 0)$ mode becomes dominant leading to the state depicted in figure 1(a). This figure shows the radial component u_r of the velocity field at a fixed radius $r = 0.75\,R_2$, i.e. in the middle of the spherical shell; bright colors indicate outward and dark colors inward motion of the fluid. This axisymmetric state exhibits four toroidal convection rolls. In our simulations, the axis of symmetry is the z-axis, but the orientation should in fact be arbitrary in the absence of rotation.

Although this state seems to be stable, careful analysis reveals that this solution is a transient state. Longtime integration shows that while the kinetic energy appears to saturate, some small modes still exhibit exponential growth. This axisymmetric pattern is indeed a stationary solution, but it is unstable. This conjecture is confirmed by the following theoretical arguments and by computing the leading eigenvalues of the Jacobian matrix treated in the next section. An essential result of the linear stability analysis in [2, 6] was that for the gap size $\beta = 1$ considered here, a single spherical mode number $l = 4$ becomes unstable at the onset of convection. Busse [7]

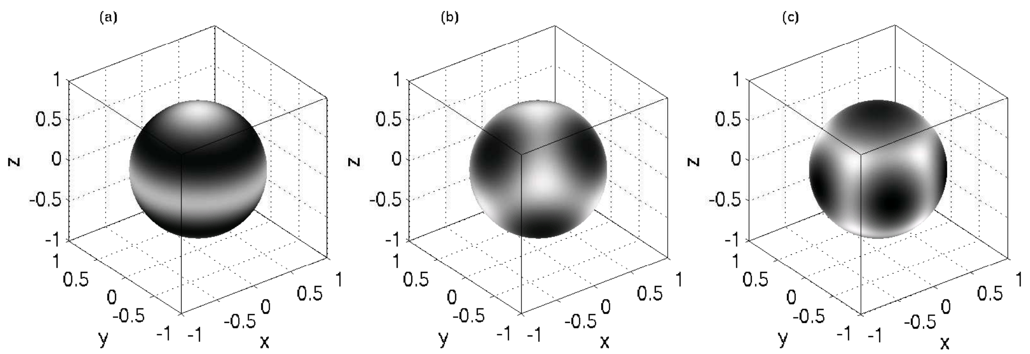

Figure 1. Radial velocity u_r of (a) axisymmetric state at Ra = 2500, (b) octahedral symmetric state at Ra = 3000 and (c) $m = 5$ state at Ra = 9000.

computed by means of a nonlinear stability analysis the bifurcating branches in the vicinity of the critical Rayleigh number for different kinds of instabilities. In particular, when the $l = 4$ mode is responsible for the onset of convection, he determined that the bifurcating branch had octahedral symmetry. In addition, Chossat et. al [8] classified symmetry-breaking bifurcations of the spherical group and characterised the bifurcation for the case in which the subgroup of one bifurcating branch is the octahedral group. Two branches bifurcate at the same critical Rayleigh number, one stable branch with the octahedral symmetry and one axisymmetric branch which is unstable. Following these theoretical arguments one can explain the scenario described above. The axisymmetric state, figure 1(a), was already discussed above. The stable branch with octahedral symmetry was found by starting from rest at a Rayleigh number of $\mathrm{Ra} = 3000$ and integrating until convergence was reached. The resulting pattern is given in figure 1(b) and, as expected, exhibits the symmetry of a cube or of an octahedron.

A further coexisting stable branch has been found for $\mathrm{Ra} > 7500$. In addition to the dominant $(4, 0)$ modes, the $(6, 5)$ modes are excited, which gives the convective pattern shown in figure 1(c). This pattern consists of five (rounded) square inflow regions around the sides and two (rounded) pentagonal inflow regions at the poles, with ten triangular outflow regions at the boundaries between the inflow regions. The pattern exhibits five-fold rotational symmetry around the z-axis (which, again, could be oriented arbitrarily) and reflection-symmetry with respect to the equatorial plane. Because of the pentagonal symmetry, we call this the $m = 5$ pattern.

For Rayleigh numbers $\mathrm{Ra} > 25000$, the convection becomes time-dependent. Preliminary investigations indicate that a Hopf bifurcation seems to generate time-periodic solutions with a subsequent transition to chaos for higher values of the Rayleigh number. However, for a complete explanation, a more accurate analysis of this transition process is required, which will be part of further investigations.

3. Bifurcation analysis

In order to better understand the bifurcation diagram, a path-following method was applied by means of which the stationary branches can be traced systematically. For this purpose, the steady states were computed by adapting the time-stepping code to perform Newton iterations. The linear system arising at each Newton step is solved by using a biconjugate gradient method. The advantage of this procedure is that, rather than inverting the Jacobian matrix, only the action of the linearized equations on the intermediate state must be computed; for more details see [5]. Using the states given in figure 1(a-c) as initial conditions, the corresponding branches were computed for both decreasing and increasing Rayleigh numbers. The result is shown in figure 2 where the kinetic energy is plotted versus the Rayleigh number.

The solid black line denotes the axisymmetric branch of state 1(a), the solid gray line the octahedral branch of state 1(b) and the dashed line the $m = 5$ branch of state 1(c). While the axisymmetric and octahedral branches could be computed in the entire region of Rayleigh number investigated, i.e. from the onset of convection at $\mathrm{Ra} = 2491$, up to $\mathrm{Ra} \leq 20000$, the convergence of the path-following program is restricted for the third branch, c.f. figure 1(c), to values of $\mathrm{Ra} > 5500$. This behavior is an indication of the possible occurrence of a turning point, below which the branch ceases to exist.

In order to determine the linear stability of the branches in figure 2 their leading eigenvalues were computed by means of the Arnoldi method [5]. Hence it could be verified that the axisymmetric state of figure 1(a), extensively discussed in the last section, is indeed unstable at $\mathrm{Ra} = 2500$. Its largest eigenvalue is positive and its second one zero. The leading eigenvalues have been calculated for the octahedral state 1(b) and the $m = 5$ state 1(c) over the parameter ranges of $3000 \leq \mathrm{Ra} \leq 20000$ and $7500 \leq \mathrm{Ra} \leq 20000$ respectively. Each state appears to be stable in these ranges. However, it should be noted that the $m = 5$ branch (shown as the dashed line in the bifurcation diagram) is initially unstable when it appears at $\mathrm{Ra} \approx 5500$.

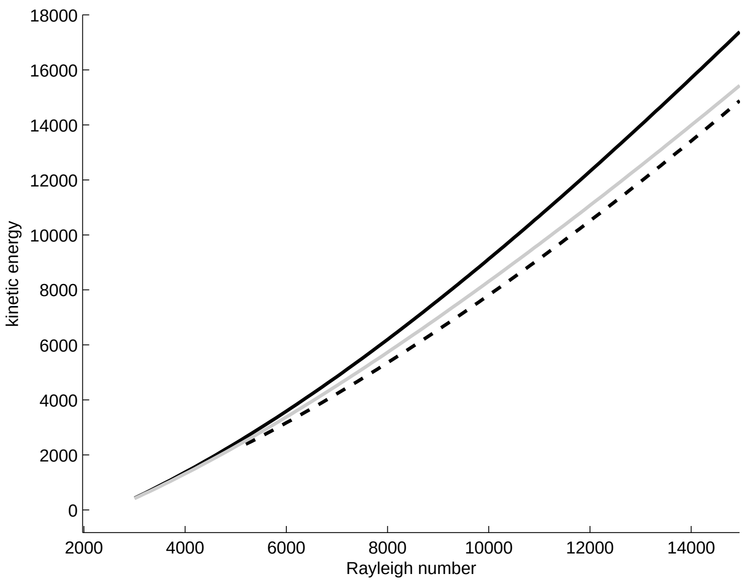

Figure 2. Steady-state branches corresponding to figure 1(a) (solid black line), 1(b) (solid gray line) and 1(c) (dashed line)

4. Conclusions

Convection in a heated spherical gap has been investigated by means of a pseudo-spectral time-stepping code as well as by path-following methods and a linear stability analysis. For the nonrotating case considered, three different convective states have been found and their stability has been determined.

Of special interest is the question of which of these states will actually be observed in the GeoFlow experiment. Since the experimental procedure is similar to that used in the simulations, i.e. the Rayleigh number is adjusted suddenly from zero, we expect that all three states discussed above will be observed. Even though the axisymmetric state is unstable, its transient is very long and so it appears to be likely to be noticed in the experiment.

Future work will focus on the detailed determination of the stability of the states obtained and of the transitions between them. Furthermore, the transitions from steady to time-dependent states and especially the route to chaos will be investigated.

References

[1] Egbers C, Beyer W, Bonhage A, Hollerbach R, and Beltrame P 2003 GEOFLOW-EXPERIMENT ON ISS Part I: EXPERIMENTAL PREPARATION AND DESIGN OF LABORATORY TESTING HARDWARE *Adv. Space Res.* **32** 171–180

[2] Travnikov V, Egbers C, and Hollerbach R 2003 GEOFLOW-EXPERIMENT ON ISS Part II: NUMERICAL SIMULATION *Adv. Space Res.* **32** 181–189

[3] Beltrame P, Travnikov V, Gellert M, and Egbers C 2006 GEOFLOW: simulation of convection in a spherical shell under central force field *Nonlin. Process GeoPhys.* **13** 413–423

[4] Hollerbach R 2000 A spectral solution of the magneto-convection equations in spherical geometry *Int. J. Num. Meth. Fluids* **32** 773–797

[5] Mamun C K and Tuckerman L S 1995 Asymmetry and Hopf bifurcation in spherical Couette flow *Phys. Fluids* **7** 80–91

[6] Travnikov V 2004 *Thermische Konvektion im Kugelspalt unter radialem Kraftfeld* PhD thesis (BTU Cottbus)

[7] Busse F H 1975 Pattern of convection in spherical shells *J. Fluid Mech.* **72** 67–85

[8] Chossat P, Lauterbach R, and Melbourne I 1990 Steady-state bifurcation with $O(3)$-Symmetry *Arch. Rational Mech. Anal.* **113** 313–376